



Aperiodic Space-Filling Geometry as a Spatial Logic

Claire DJANG  and Stefano ARRIGHI 

Studio Olafur Eliasson
Christinenstraße 18-19, 10119 Berlin, Germany
claire.djang@olafureliasson.net

Abstract

This paper presents a computational tool for generating aperiodic, space-filling quasicrystal assemblies using golden rhombohedra and zonohedral tiles. Implemented in Rhino–Grasshopper, the plugin applies recursive subdivision algorithms to fill bounded volumes, surfaces, or curves with non-periodic three-dimensional tilings. It outputs transformation data for each tile instance, enabling efficient substitution with custom geometry and supporting designs that scale to over 100,000 discrete elements. While digital tools have incorporated periodic space group symmetries, aperiodic systems remain underdeveloped in architectural workflows despite their potential for non-repetitive spatial order. We situate our tool within a lineage of architectural engagement with space-filling geometry, referencing the work of Buckminster Fuller, Anne Tyng, and Einar Thorsteinn. In particular, we realize Thorsteinn’s unresolved investigations into golden rhombohedral assemblies, offering a computational implementation of the geometric systems he explored conceptually. We further contextualize this work through several case studies by Studio Olafur Eliasson that demonstrate a progression from periodic crystalline logic to quasicrystal-inspired aperiodic structures. By formalizing aperiodic tiling within a parametric design environment, this tool expands the technical and conceptual capacity of space-filling logic and enables new applications for non-periodic spatial systems.

Keywords: Aperiodic Tiling, Quasicrystals, Grasshopper, Discrete Design

1. Introduction

Space-filling polyhedra have long offered architects a framework for structuring form and space through geometric logic. Throughout the 20th century, a number of designers turned to polyhedral systems not only as formal devices, but as generative principles capable of shaping architectural experience. In the 1960s and 1970s, a crystallographic tendency in architecture emerged as a distinct design subculture. Andrew Witt describes this movement as extending crystallography beyond building form into a broader philosophical understanding of reality (Witt, 2023). This movement was marked by modular experiments, large-scale geometric models, and an optimistic faith in the architectural potential of polyhedral structure. Although Witt observes that this tradition largely receded by the end of the 1980s, its principles have resurfaced in more recent projects such as the Beijing National Swimming Center (Pearson, 2008). In this paper, we follow this thread into contemporary design practice, focusing on a set of projects developed by Studio Olafur Eliasson. The

studio's collaborations with architect and mathematician Einar Thorsteinn led to a series of installations and architectural proposals that pushed crystalline logic toward greater spatial complexity and irregularity. These case studies highlight a shift from regular repetition to quasi-ordered variation, and from fixed modules to responsive systems of transformation.

Building on this history, we aim to extend the use of space-filling polyhedra in design into a contemporary architectural context, where computation, fabrication, and geometry converge. As the complexity of geometric constructions increase, advanced software tools become essential for visualizing and understanding three-dimensional patterns. The technical advancements provided by a parametric environment allow treatment of individual geometries not only as precisely-defined objects in space, but also as part of a data structure that can be organized and expanded upon. The Grasshopper (Robert McNeel & Associates, 2023) component library HORTA (McLemore, 2020) implements the construction of three-dimensional symmetric assemblies in design software, following the international system developed by crystallographers since the early 20th century. This covers all 230 space groups, mathematically proven to be all unique configurations of repetitive geometries that can arise within periodic lattices in three dimensions.

Quasiperiodic assemblies in three dimensions have not been, until now, implemented in any comparable way. We present a new computational tool that generates three-dimensional quasicrystalline assemblies based on rhombohedral and zonohedral tiles. The plugin enables new forms of design inquiry grounded in non-repeating, yet highly ordered, spatial systems. As Witt notes, the decline of architectural crystal subcultures in the 1980s coincided ironically with significant advances in computational power. Thorsteinn also reflected that 3D geometric experimentation had fallen out of fashion for a number of decades (Thorsteinn & Eliasson, 2002). Through our tool, we advocate for renewed interest in the potentials of crystalline geometry, positioning our work at the intersection of mathematics, natural sciences, computational design and architecture.

2. Background

A space-filling polyhedron is a polyhedron that can be used to generate a tessellation of space (Weisstein, 2025). The cube is the only single Platonic solid possessing this property, but combinations of regular tetrahedra and octahedra fill space, as do other combinations of octahedra, truncated octahedra, and cubes. The tetrahedral-octahedral honeycomb, where two Platonic solids operate as complementary space fillers, was used by Buckminster Fuller in his octet truss design (Fuller, 1975) and also in Anne Tyng and Louis Kahn's City Tower project, which Tyng compared to Watson and Crick's DNA model (Kahn & Tyng, 1952).

In her work, Tyng developed recursive subdivisions of Platonic solids to articulate hierarchies of symmetry, connecting cosmic conceptions of structure to the embodied logic of architectural form (Tyng, 1969). Einar Thorsteinn extended this inquiry but moved beyond the stable symmetries of Platonic solids toward the unresolved complexity of aperiodic geometries. Fascinated by golden rhombohedra and their potential for non-repeating spatial organization, he notes that the discovery of quasicrystals in 1984 prompted a shift in cultural interest in 3D geometry and fivefold symmetry in particular (Thorsteinn & Eliasson, 2002). He observed that two types of golden rhombohedra could pack together to fill a rhombic triacontahedron, but did not discover a way to expand this structure to infinitely fill space.

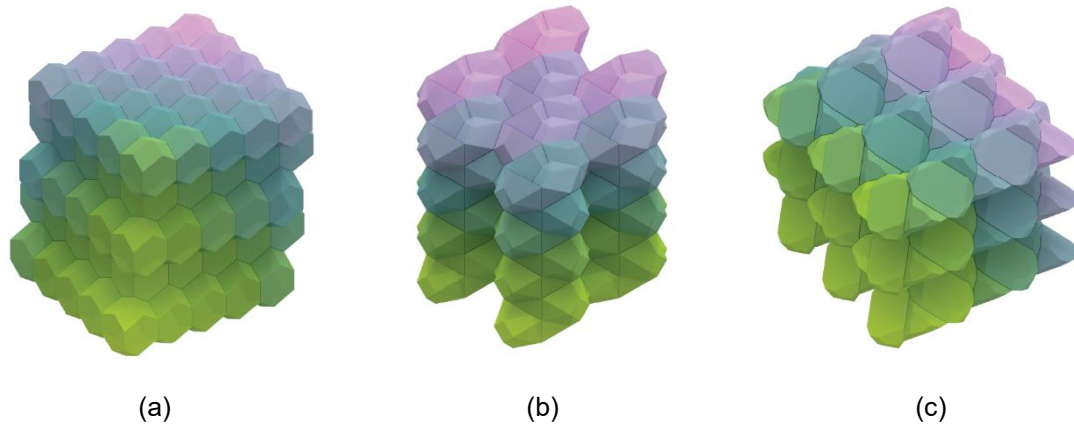


Figure 1. A selection of three different space-filling polyhedra, showing how each module stacks together with identical copies of itself to fill space without any gaps. The elongated dodecahedron, the bisymmetric hendecahedron, and a heptadecahedron derived from the Laves graph are shown.

A more recent architectural example demonstrates how the use of space-filling geometry in architecture has tended to move toward greater complexity and perceived randomness. The facade and structural logic of the Beijing National Aquatics Center is based on the Weaire–Phelan structure, a space-filling geometry derived from foam and soap bubble clusters, which optimizes the division of space into cells of equal volume with minimal surface area. It consists of a packing of two polyhedral cell types: one with 14 faces (a truncated octahedron-like shape) and another with 12 faces (a modified dodecahedron). Though the underlying mathematical structure is still periodic, the design team expressed a desire for the bubble pattern to seem random, not repetitious (Pearson, 2008).

The *Façade for Harpa Reykjavik Concert Hall and Conference Centre* (Eliasson, 2005–2011), designed by Studio Olafur Eliasson with Henning Larsen, remains one of the few examples of a crystalline logic translated into a large-scale architectural envelope. In the 1980s, Thorsteinn developed a three-dimensional polyhedron he called the ‘quasi brick.’ It is a twelve-sided solid composed of parallelograms and hexagons, also known as an elongated dodecahedron, one variation of which is shown in Figure 1a. Unlike the more regular rhombic dodecahedron, the module allows for variability in the proportion of its side lengths while still stacking periodically. Inspired by research into quasicrystals, Thorsteinn refined the exact proportions of the quasi brick such that its form contained a combination of both regular and irregular faces. For the Harpa project, the design team was interested in the idea of using both aperiodic and regular tiling to constellate these building blocks (Kuo, 2018). Though technically not achieved in the geometry itself, the concept of aperiodicity is expressed through varied materials and sectional cuts through the tessellating form to reveal a nonstandard structure. The façade presents a suggestion of organic growth through modular assembly.

At a smaller scale, *A harmonious cycle of interconnected nows* (Eliasson, 2023) is another Studio Olafur Eliasson project that features a space-filling assembly. The sculptural installation is made from thousands of repeating modules and comprises four spiraling forms that visualize motion, time, and gravitational flow. The elements, cast in recycled zinc recovered from fly ash, are based on the space-filling bisymmetric hendecahedron, an 11-faced polyhedron of rhombi, kites, and triangles (Figure 1b).



Figure 2: Façade for Harpa Reykjavik Concert Hall and Conference Centre. Reykjavik, 2011.
Photo: Olafur Eliasson



Figure 3: A harmonious cycle of interconnected nodes, 2023. Azabudai Hills Mori JP Tower Office Lobby, Tokyo Japan – 2023. Photo: Kioku Keizo

This more recent project from Studio Olafur Eliasson continues with the use of space-fillers, this time, where the modular aggregation appears less regular due to the multiple orientations of the tile (compare Figure 1b to 1a). Further irregularity is achieved through the overall forms of the sculpture. The spirals are derived from Clelia curves, generated by modifying angular velocity ratios to produce contraction effects toward a spherical center. The juxtaposition of the tile aggregation logic with the continuity of space curves creates an effect where regular repetition is not clearly visible. The growth of the assembly changes along trajectories independent from the discrete tiling logic.

More recently, aperiodic tiling principles have been applied to architectural façades through reinterpretations of the two-dimensional Penrose tiling, one of the most well-known examples of non-repetitive order. The RMIT Storey Hall in Melbourne (ARM Architecture, 1995) features a tessellated façade based on this pattern, producing a distinctive, non-repeating surface. The Atmospheric Wave Wall (Eliasson, 2020) further translates the Penrose rhombic base tiles into a “spherical-portion” system, generating a shimmering aluminum relief whose geometry shifts with changing light and perspective. Similarly, Elegant Embellishments’ façade for the Hospital Manuel Gea González in Mexico City employs an aperiodic pattern derived from the same two-dimensional logic to create a self-cleaning, depolluting surface. Only a few examples, and primarily at smaller scales, extend this logic into three-dimensional space-filling assemblies, such as ArandaLasch’s Quasi series (Aranda & Lasch, 2005), which explores quasicrystal geometries through modular, non-repetitive aggregations of polyhedra.

3. Methods

3.1. Quasicrystals: a Penrose Tiling in 3D

The icosahedral packings of quasicrystals can be seen as the 3D equivalent of the 2D aperiodic Penrose tiling. We may construct tilings with two rhombohedral tiles (Figure 4, left) to generate 3D packings with icosahedral symmetry. These tiles are the *acute rhombohedra* A_6 and the *oblate rhombohedra* O_6 . Steinhardt et al. (1986a, 1986b) proposed a theoretical description for quasicrystal construction that consists of four distinct tiles (Figure 4, right) rather than the two rhombohedra. All are golden isozonohedra. The acute rhombohedra A_6 is one of the four tiles. The other three tiles are the *rhombic (Bilinski) dodecahedron* B_{12} , the *rhombic icosahedron* F_{20} , and the *rhombic triacontahedron* K_{30} . Note that the three larger zonohedra may be also subdivided into packings of only A_6 and O_6 tiles.

The work of Alexey E. Madison (2015), described in his article *Substitution rules for icosahedral quasicrystals*, reveals a substitution algorithm for constructing the same 3D patterns previously explored by Steinhardt and others. Madison’s paper describes rules defining how each of the four tiles may be substituted by large clusters of the same four tiles scaled down, allowing infinite expansion of the pattern through recursion. These substitution rules, including the scaling down operation on the tiles, are known as *deflation rules*, whereas the term *inflation* refers to subsequently scaling the clustered tiles up to match their original size. See our video (Djang, 2023) for more details and visualizations of this recursive method. The deflation scale factor of φ^3 (approximately 4.236) means that a relatively large number of

tiles are already generated after a single iteration of the deflation operation: the A_6 , B_{12} , F_{20} , and K_{30} tiles are each substituted by 46, 121, 277, and 533 tiles respectively.

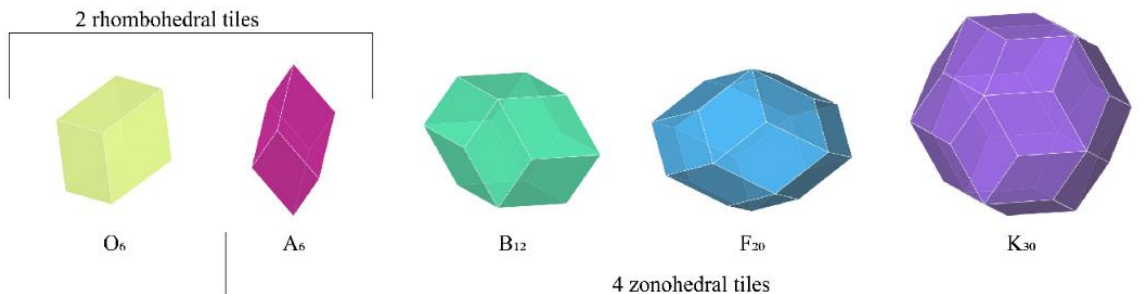


Figure 4: The five golden isozonohedra. The first two, O_6 and A_6 , are the two types of rhombohedra that form rhombohedral (“two-tile”) space-filling quasicrystal packings. The last four, including A_6 , are the four zonohedra that may also form (“four-tile”) space-filling quasicrystal packings.

3.2. The Grasshopper Plugin

Our Rhino-Grasshopper tool for aperiodic tiling (Figure 5) offers flexible input parameters and can produce diverse 3D quasicrystalline configurations. The core “four-tile” module constructs patterns from the four zonohedral tiles, generating four separate sets of transformation data. Each entry in these sets is a 4×4 matrix representing a rigid transformation in Euclidean 3-space, which may combine rotations, translations, and reflections. The tool also outputs the corresponding base tile geometries as 3D meshes at the scale defined by the user. While the base meshes remain unchanged aside from scaling, users have the option to substitute them with custom geometries (Figure 9). The transformation matrices vary according to the user’s input, and with a standard Grasshopper transformation component, each tile is copied and transformed according to its associated matrix set.

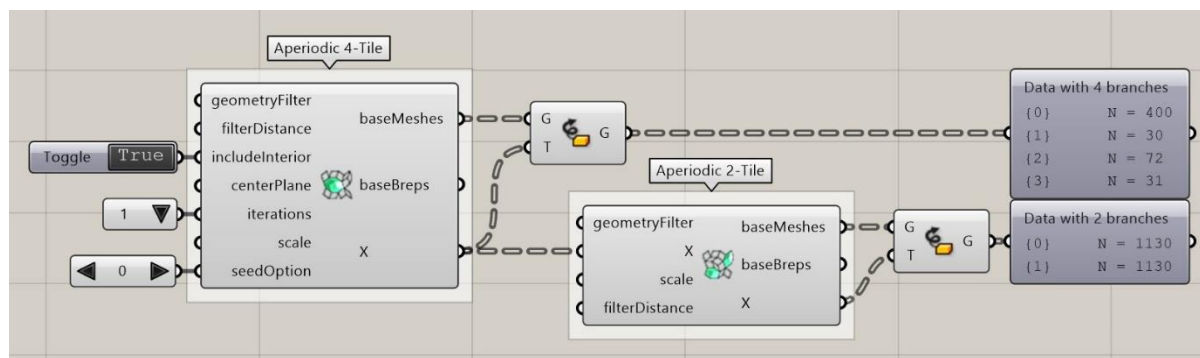


Figure 5: Screenshot of the custom four-tile and two-tile components in Grasshopper 3D, showing input and output parameters. Transformations denoted by X are used to generate tiling patterns

The tool also includes a secondary “two-tile” module that builds on the results of the four-tile component. Transformation outputs from the four-tile module are fed into the two-tile component and combined with additional transformations needed to position the two rhombohedral tiles within each of the four original base tile types, effectively replacing or

subdividing them. The resulting two rhombohedral tiles, A_6 and O_6 , can then be applied with the transformation lists generated by the two-tile module to produce a quasicrystalline packing consisting solely of these two tiles. Consequently, all tilings are initially created using the four-tile component and may then be optionally refined with the two-tile module.

The total number of tiles grows exponentially with each iteration. A single deflation of the K_{30} tile (Figure 6b) generates 533 zonohedral tiles, while a second deflation (Figure 6c) produces 45,873 tiles. The two-tile configurations illustrated in Figures 6d and 6e are created by substituting the zonohedral tiles from Figures 6b and 6c with the two rhombohedral tiles, resulting in 1,860 and 154,040 tiles, respectively.

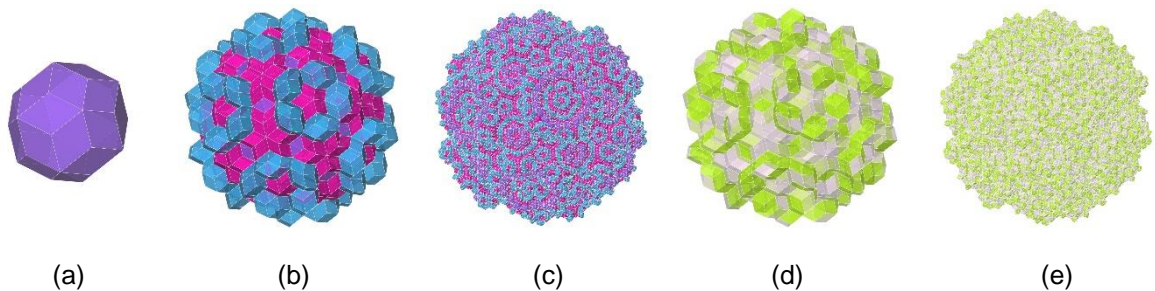


Figure 6: Digital models generated by our tool, showing the deflation of the K_{30} tile and other modifications: (a) the base K_{30} tile, (b) deflation after 1 iteration (533 tiles), (c) deflation after 2 iterations (45,873 tiles), (d, e) replacement of the four zonohedral tiles with the two rhombohedral tiles

3.3. Implementation

For most tiles in the pattern, the deflation configuration does not maintain the same symmetries as the original tile. The deflated clusters from the A_6 , B_{12} , and F_{20} tiles may be oriented in one of two possible opposing directions relative to the initial geometry (Figure 7), but only one orientation produces a valid tiling. In our implementation, it was therefore necessary to determine exact positions of the deflation planes in 3D space, rather than relying solely on the tile placements illustrated by Madison (2015). Across all four sets, this resulted in a total of 977 individual planes.

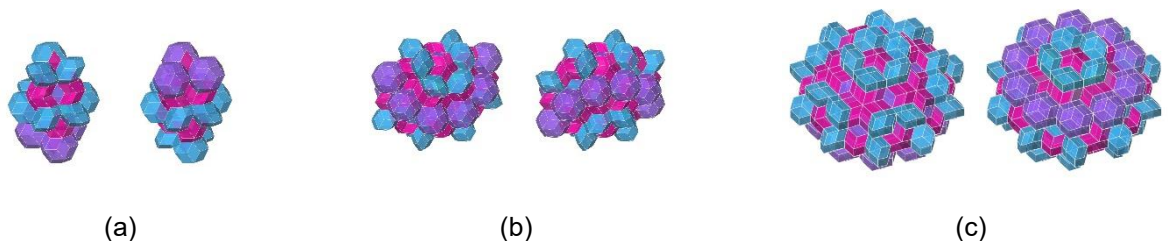


Figure 7: Possibilities for deflating a non-oriented tile: (a) A_6 deflation according to one possible orientation and the other possible (opposing) orientation (b) B_{12} deflation (c) F_{20} deflation. Note: while no B_{12} tiles are visible, they are present on the interior of the clusters.

Madison did not provide orientation details or Cartesian coordinates that could be directly used. To determine each tile's orientation, we leveraged the fact that every tiling consists of two alternating vertex types, with no edges connecting equivalent vertices, and that the inflation/deflation process preserves these vertex types (Madison, 2015, p. 5748). Consequently, any two tiles sharing a vertex must be aligned to match at that point during deflation. This principle enabled the sequential placement of tiles and orientations within our encoded deflation rules, implemented through reflections, rotations, and mesh operations in the RhinoCommon API using C#.

3.4. Features and Options

Once the center points and vector axes of the 977 deflation orientation planes were established, this global data was stored and a recursive process was implemented. Users can specify an integer number of *iterations* to control the depth of recursion. Each iteration applies an additional layer of plane-to-plane transformations: a set of planes (organized into four lists) is transformed according to the deflation rules, producing four new lists of planes that are then compiled and reorganized for the next iteration. These transformations accumulate with each successive iteration, enabling increasingly complex tiling patterns.

The recursive process can expand a small initial tile configuration into larger tilings, but the starting orientation planes must conform to the tiling rules. In our tool, we defined controlled base cases, referred to as *seed options*. For the four-tile pattern, there are exactly three complete packings with a single center exhibiting icosahedral point symmetry that fill 3D Euclidean space (Socolar & Steinhardt, 1986, p. 636; Madison, 2015, p. 5749). These three configurations are preferred due to their distinct structures and their ability to produce icosahedral symmetry. Each option is generated using one of the following seed configurations: the default begins with a single K_{30} tile (Figure 6a); the second starts with a star of twenty A_6 tiles, which are subsequently surrounded by K_{30} tiles after deflation/inflation; the third also starts with twenty A_6 tiles, but with flipped orientations relative to the second option, so that the next layer after deflation/inflation is surrounded by F_{20} tiles. Selecting a different seed option alters the formation of the base tiling while maintaining icosahedral symmetry and user-selected options such as bounding geometry (Figure 8).

4. Results

4.1. Use of the Geometry Filter

During deflation, duplicate tiles are created along shared faces and edges of the original pre-deflated pattern (Madison, 2015, p. 5747) because the border tiles of each deflation rule extend beyond the original tile boundaries. Our tool automatically identifies and removes these duplicates at each recursion step. Nevertheless, the recursive process still produces configurations with uneven, fractal-like edges (Figure 6c). To shape the resulting tilings into smooth forms, such as spheres, boxes, or space curves (Figure 8), it was necessary to implement a sculpting and trimming process.

Another challenge arose from the large number of geometries generated. Even representing each tile as a simple mesh, running more than two iterations led to long computation times.

We addressed both issues using a *geometry filter*. By specifying any 3D curve, surface, or volume (including meshes) in Rhino, the tool includes only tiles within a defined tolerance of the input geometry, controlled via the *filter distance* parameter. This approach also enables breaking the controlled icosahedral symmetry set by the initial seed options. A Boolean option, *include interior*, lets users decide whether to retain tiles inside a closed geometry or to create a hollow formation.

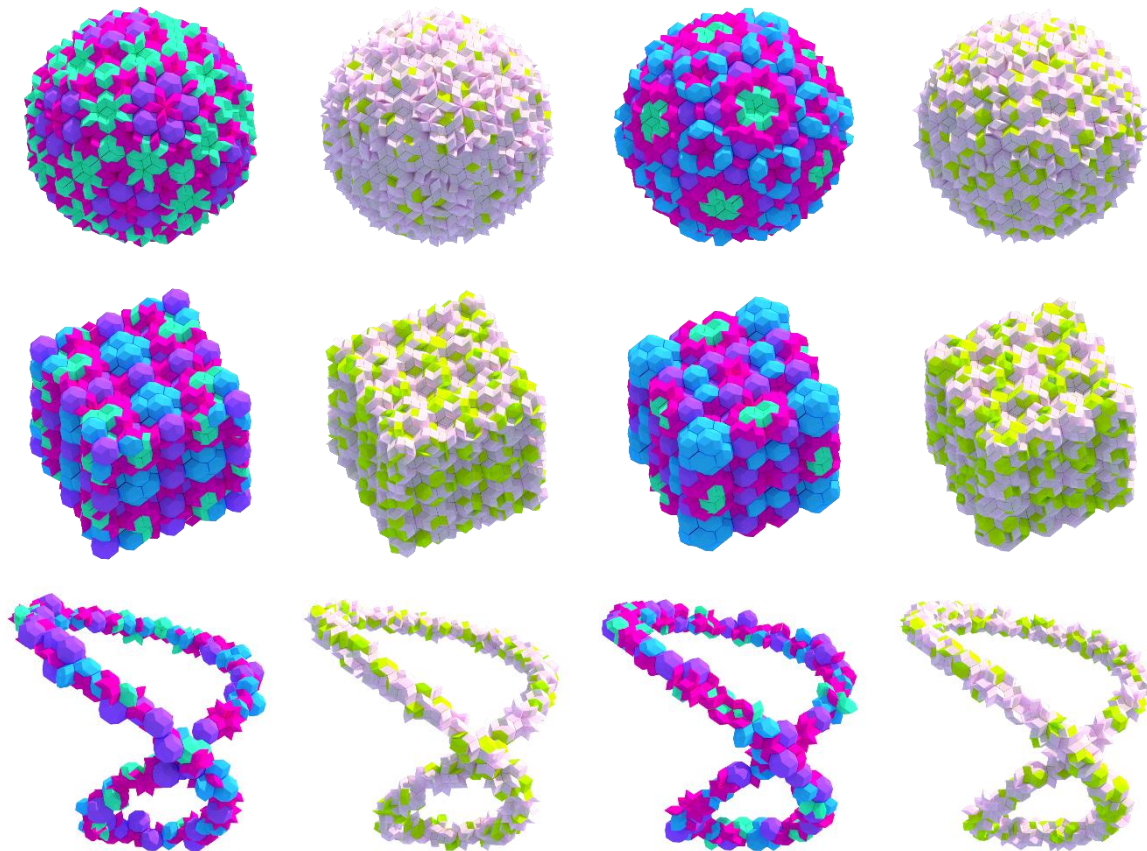


Figure 8: Each row shows tilings bounded by a different geometry filter: a sphere, a cube, and a space curve. Each column alternates between the four-tile and two-tile methods. The four-tile configurations exhibit icosahedral symmetry, which is no longer present when they are converted to two-tile configurations. Two different seed options are shown (left two columns vs right two columns).

The geometry filter additionally improves computational efficiency by pruning tiles early in the recursive process. By scaling the filter down in proportion to the deflation factor (ϕ^3) at each iteration, tiles and planes outside the tolerance are excluded before further transformations. This early filtering significantly reduces the total number of operations, enabling the tool to generate larger-scale tilings with more iterations of recursion.

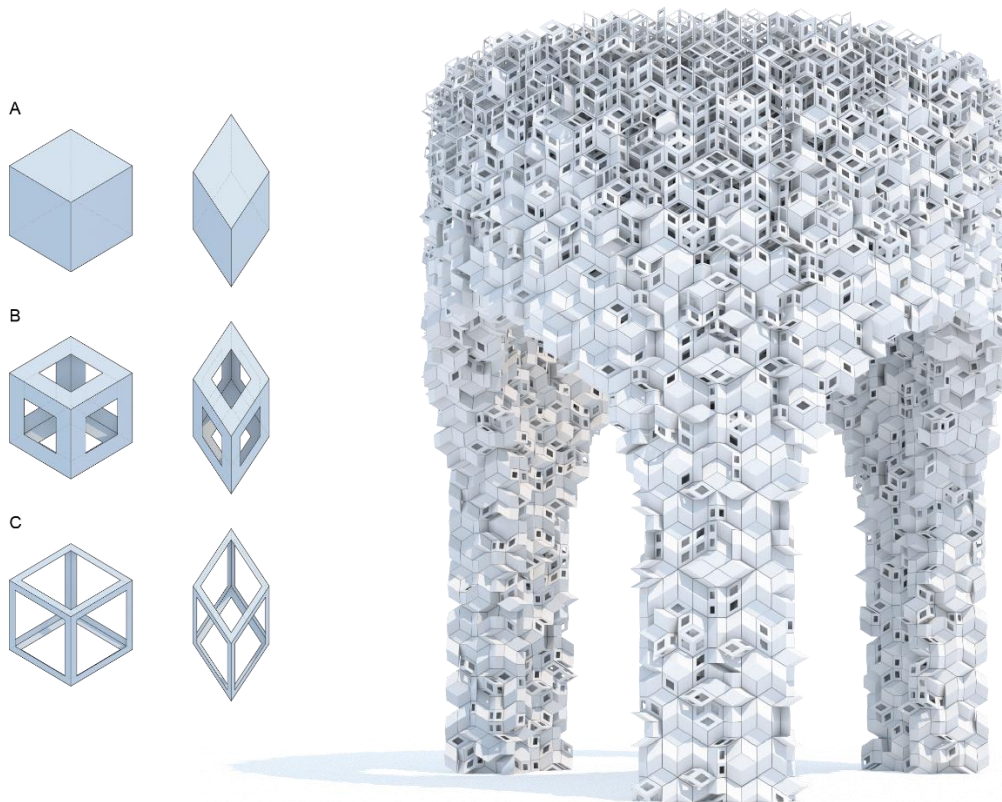


Figure 9: The tool enables easy substitution of the two base rhombohedral tiles with custom geometric variations. The images illustrate how a gradient-like pattern can be achieved by introducing three variations for each tile type.

4.2. Replacing Tiles with Custom Geometry

Because the tool outputs transformation data rather than the tiles themselves, any geometry can be substituted for the tiles to create new configurations that preserve an aperiodic structure without necessarily being space-filling.

The fundamental solid rhombohedral blocks could be replaced with truncated or curved forms, for example, with variations in material, color, structural or ornamental features (Figures 9 and 10) and a range of tile types may be assigned parametrically according to specific design constraints. Figure 9 illustrates a configuration in which the two rhombohedral tiles vary according to their distance from the arches of the underlying massing, producing a gradual transition rationalized into three different porosity levels for each base tile.

This demonstrates how differentiation between tile types, whether based on performance or other design constraints, can be achieved and explored while retaining the discrete structure of aperiodic tiling. By separating transformation logic from geometry, the system becomes a flexible framework for material, structural, or fabrication strategies at architectural scale.

4.3. Realized Projects

Uncertainty lens (Eliasson, 2025), exhibited in 2025 at neugerriemschneider gallery, translates principles of aperiodic space-filling rhombohedra into a physical sculpture. It is a built application of our tiling tool. The work contains a suspended sphere approximately one meter in diameter, representing a cluster of 110 rhombohedral tiles. Rather than treating tiles in the pattern as solid blocks, in this case, we focused only on vertices and edges of the pattern to form a structure of nodes and connecting rods. The construction relied on modular assembly: repeating nodes allowed the creation of 30 identical modules, which were then joined into 12 distinct fragments before being combined into the full sphere. Selected facets are highlighted using transparent panes that interact with light and perspective. This built artwork demonstrates how aperiodic tilings generated by the tool can be realized in physical design.

4.4. Geometric Explorations

Operation of our tool within the Grasshopper 3D environment provides a platform for further investigation of the complex structure of quasicrystals. We can explore and animate operations such as rotations, explosions, and sectional cuts of various 3D packings. Some of these visualizations are available in our video (Djang, 2023). Continuing these explorations, we find that these tiling aggregations exhibit unique geometric properties, particularly when considering the discrete yet varied set of orientations of the edges, faces, and tiles within the pattern.

In one study (Djang, 2025) we show how certain polyhedra, defined as the outer surface boundary of spherical clusters generated by our tool, bear close resemblance to zonohedra in terms of their geometric properties, as faces may be grouped into six zones with related orientations. As a result, these spheres may be constructed from overlapping continuous folded bands of paper or other flat material. The bands, in both their folded and unfolded state, follow repeated and predictable patterns with potential for an efficient production logic.

Aperiodic tilings enable a single geometric unit to appear in a wide range of orientations within a pattern, producing configurations that are visually unexpected compared to the fixed, repetitive orientations characteristic of periodic tilings. In Figure 10a, we replace the base rhombohedral tiles with two node-like units, each composed of the three axes connecting opposing faces of the original tiles. For each of the two substituted tile types, a difference in material highlights a single axis. This difference, which could also represent a formal or structural deviation in the module, begins to break the original symmetry of the tiling unit, still without changing its aggregation logic.

The generated structure maintains connectivity between adjacent tiles only at the face center points of the original tiles. The pattern contains no gaps in tiles, so the axes of connected tiles form continuous intersecting polylines through the pattern, not unlike the overlapping folded bands from our previous study. We begin to see the interwoven nature of the three-dimensional aperiodic grid, in all its many orientations.

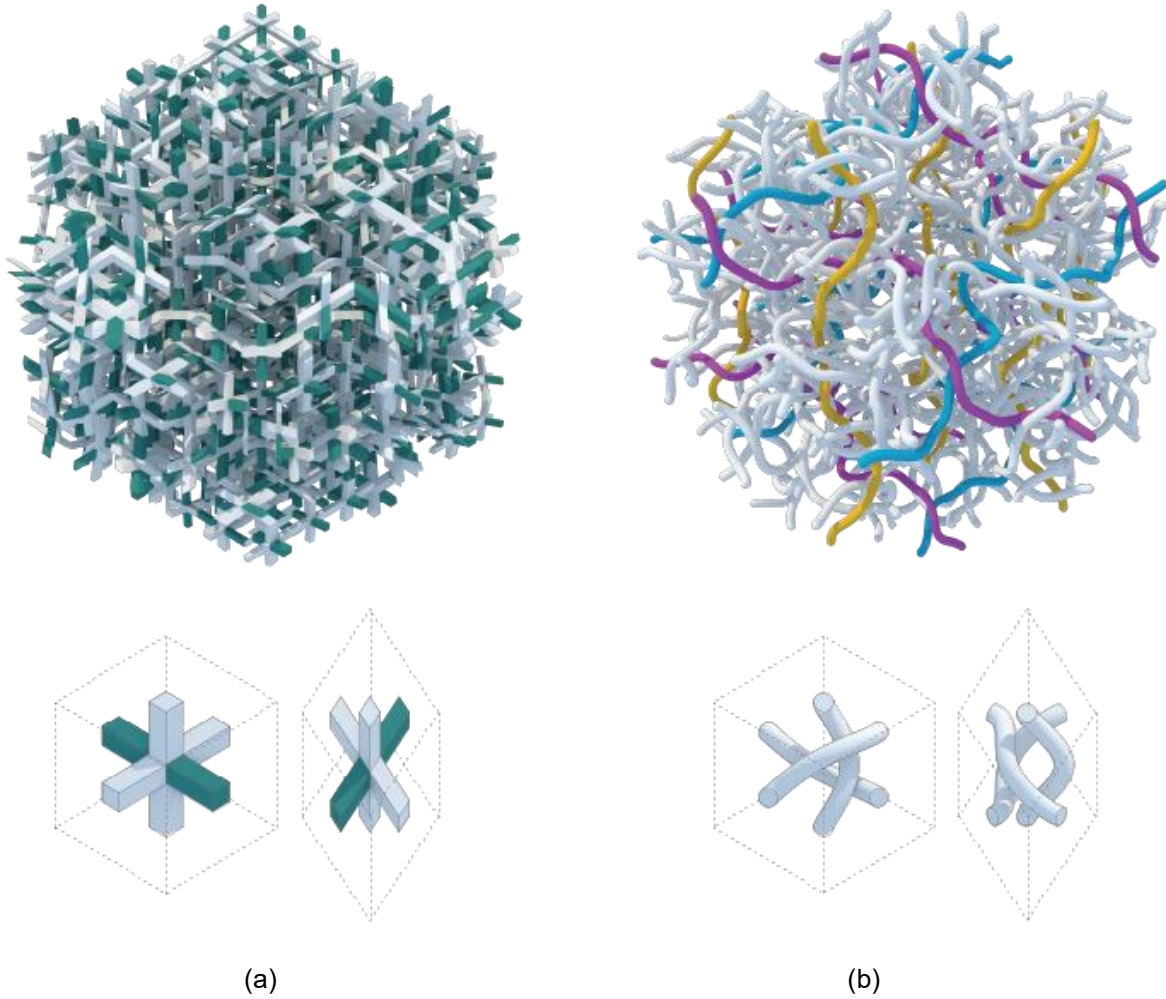


Figure 10: Exploration of tile substitution for the two base rhombohedral tiles: (a) replacement of the base tiles with node-like units composed of three intersecting axes; (b) an interwoven reinterpretation that introduces continuous connections while avoiding thread intersections across the aperiodic field

A second study furthers this investigation. As illustrated in Figure 10b, the two rhombohedral tiles are replaced with an interwoven configuration that maintains continuity across the aperiodic field while avoiding collisions between threads. This example highlights three distinct orientation groups of connected tiles, illustrated through three colors. These threads represent a continuous movement through tiles in the original pattern that always share sets of parallel faces. In total, there are 15 possible orientations of faces in the original pattern, following all orientations of the faces of the rhombic triacontahedron, and the resulting configuration in Figure 10b contains threads that may be organized into 15 orientation groups. These woven structures can be generated without collision, enabling a coherent organization of continuity and directionality across the aperiodic field while preserving the underlying geometric logic of the tiling.

5. Reflection

The spatial framework offered by quasicrystals allows for new aesthetic and material possibilities. Though constructed from only two or four tiles, the recursive logic produces highly differentiated fields. Because face types and orientations are finite and predictable, the system supports both mass production (e.g., node kits) and unique forms. The possibility of parametric substitution also allows for differentiation of porosity, structure, or material across the pattern.

Future work includes fabrication studies, deployment in architectural skins and partitions, and integration with robotic or rule-based construction systems. We also plan to release the plugin as an open-source design tool.

6. Conclusion

The exploration of space-filling polyhedral systems in architecture has long been intertwined with broader questions of structure, scale, and spatial imagination. From the recursive hierarchies of Anne Tyng to the quasi-structural logic of Einar Thorsteinn, geometry has served not merely as a formal language but as a conceptual framework for inhabiting space. Recent projects engaging quasicrystalline assemblies, such as those developed within Studio Olafur Eliasson, demonstrate the continued relevance of these inquiries in contemporary design practice. Building on this lineage, the computational framework introduced in this paper offers a means of operationalizing aperiodic order in design workflows, enabling recursive spatial systems that are scalable, non-repeating, and architecturally expressive.

Rather than treating geometry as static pattern or symbolic reference, this approach emphasizes its generative and systemic potential. By combining recursive tiling strategies with customizable formal substitution, the framework supports a shift toward complexity-through-logic, an architecture of difference without randomness, structure without repetition. In this sense, the recursive processes used in aperiodic space-filling geometries can be read as computational morphogenesis, where complexity arises from the internal logic of the system rather than external imposition. In doing so, it advances a design philosophy in which space-filling geometry becomes not only a mathematical curiosity, but a strategy for contemporary architectural form and experience.

Acknowledgements

The authors thank Studio Olafur Eliasson for the constant inspiration and for supporting this research.

References

- Aranda, B & Lasch, C. (2005). *Pamphlet architecture 27: Tooling*, Princeton Architectural Press.
- ARM Architecture. (1995). *Storey Hall, RMIT University* [Building façade and interior renovation based on Penrose tiling]. Melbourne, Australia.
<https://armarchitecture.com.au/projects/rmit-storey-hall-and-green-brain/>
- Djang, C. (2025). Icosahedral quasicrystal folded paper strip spheres. *Proceedings of Bridges 2025: Mathematics and the Arts* (pp. 555–558).
<https://archive.bridgesmathart.org/2025/bridges2025-555.html>
- Djang, C. (2023). Quasicrystals in an age of digital design. *2023 Bridges Conference Short Film Festival*. <https://gallery.bridgesmathart.org/exhibitions/2023-bridges-conference-short-film-festival/claire-djang>
- Eliasson, O. (2005–2011). *Facades of Harpa Reykjavik Concert Hall and Conference Centre* [Facade of steel, glass, LED lights]. Reykjavik, Iceland. <https://olafureliasson.net/artwork/facades-of-harpa-reykjavik-concert-hall-and-conference-centre-2005-2011/>
- Eliasson, O. (2020). *Atmospheric wave wall* [Aluminum façade, University of Iowa, U.S.]. University of Iowa Stanley Museum of Art.
<https://olafureliasson.net/artwork/atmospheric-wave-wall-2020/>
- Eliasson, O. (2023). *A harmonious cycle of interconnected nows* [Suspended spiral sculptures of recycled zinc alloy]. Tokyo, Japan. <https://olafureliasson.net/artwork/a-harmonious-cycle-of-interconnected-nows-2023/>
- Eliasson, O. (2025). *Uncertainty lens* [Installation of PET, PVC, brass, motor, electrical ballast]. Neugerriemschneider, Berlin, Germany. <https://olafureliasson.net/artwork/uncertainty-lens-2025/>
- Fuller, R. B. (1975). *Synergetics: Explorations in the geometry of thinking*. Macmillan Publishing Co.
- Kahn, L. I., & Tyng, A. (1952). *Philadelphia City Tower Project* [Unbuilt architectural project]. Architectural Archives, University of Pennsylvania, Philadelphia, PA, United States.
- Kuo, M. (2018). Experience. In A. Engberg-Pedersen (Ed.), *Olafur Eliasson: Experience* (pp. 1–60). Phaidon Press.
- Levine, D., & Steinhardt, P. J. (1986). Quasicrystals. I. Definition and structure. *Physical Review B*, 34(2), 596–616. <https://doi.org/10.1103/PhysRevB.34.596>
- Madison, A. E. (2015). Substitution rules for icosahedral quasicrystals. *RSC Advances*, 5(8), 5745–5753. <https://doi.org/10.1039/C4RA09524C>
- McLemore, D. (2020). Space group symmetry generation for design. In *ACADIA 2020: Distributed proximities / Volume I: Technical papers* (pp. 648–657).
<https://doi.org/10.52842/conf.acadia.2020.1.648>
- Pearson, C. A. (2008, July). National Swimming Center, Beijing, China. *Architectural Record*. <https://www.architecturalrecord.com/articles/8111-national-swimming-center>

- Robert McNeel & Associates. (2023). *Rhinoceros 3D and Grasshopper* (Version 8.0) [Computer software]. <https://www.rhino3d.com/>
- Socolar, J. E. S., & Steinhardt, P. J. (1986). Quasicrystals. II. Unit-cell configurations. *Physical Review B*, 34(2), 617–647. <https://doi.org/10.1103/PhysRevB.34.617>
- Thorsteinn, E., & Eliasson, O. (2002). *To the habitants of space in general and the spatial inhabitants in particular*. Bawag Foundation.
- Tyng, A. (1969) Geometric extensions of consciousness. *Zodiac*, 19, 130-161.
- Weisstein, E. W. (2025). Space-filling polyhedron. *MathWorld—A Wolfram Web Resource*. <https://mathworld.wolfram.com/Space-FillingPolyhedron.html>
- Witt, A. (2023). *Formulations: Architecture, mathematics, culture* (ch. 10, “Crystal Collectives”). MIT Press.